Electronic Supplementary Information

Methylene spacer regulated variation in molecular and crystalline architectures of cobalt(III) complexes with reduced Schiff base ligands: A combined experimental and theoretical study

Abhisek Banerjee, Antonio Frontera*, Shouvik Chattopadhyay*

[a]*Department of Chemistry, Inorganic Section, Jadavpur University, Kolkata - 700032, India. E-mail: shouvik.chem@gmail.com*

[b]*Department of Chemistry, Universitat de les IllesBalears, Crta de Valldemossa km 7.5, 07122 Palma de Mallorca (Baleares), SPAIN*

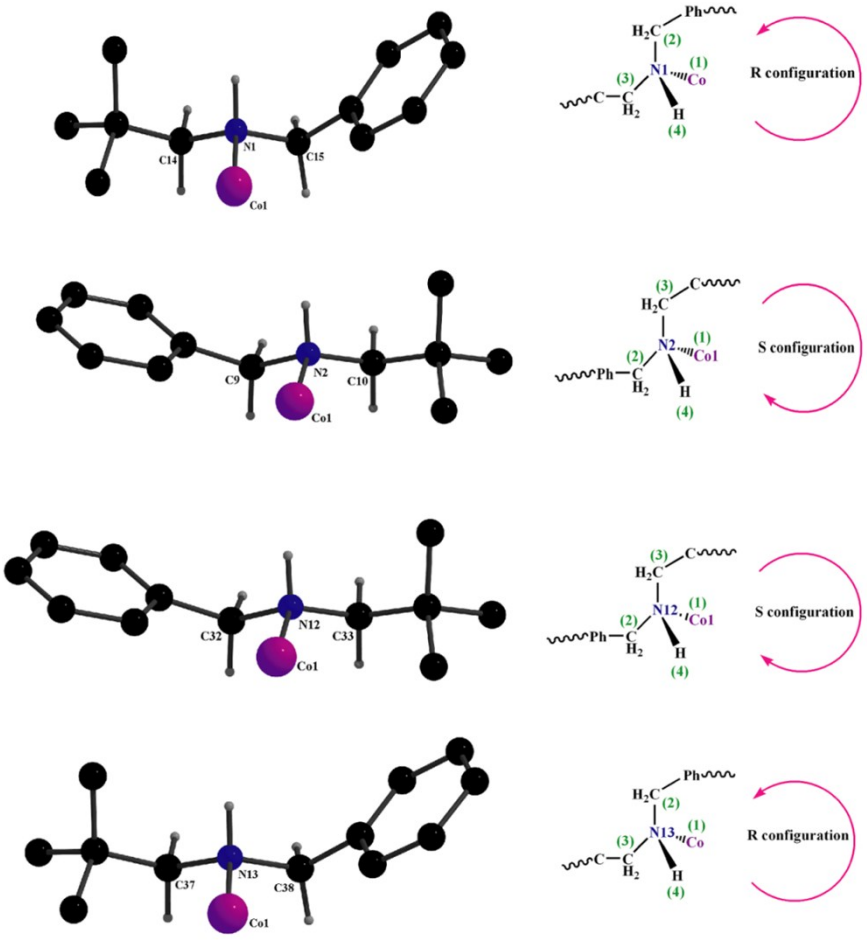

Figure S1: Configuration of chiral centres in Complex 2

Hirshfeld Surface Analysis

Hirshfeld surfaces[1-2] and the associated two-dimensional (2D) fingerprint[3-5] plots were calculated using Crystal Explorer,[6] with bond lengths to hydrogen atoms set to standard values. [7] For each point on the Hirshfeld isosurface, two distances, d_e (the distance from the point to the nearest nucleus external to the surface) and d_i (the distance to the nearest nucleus internal to the surface), are defined. The normalized contact distance (d_{norm}) based on d_e and d_i is given by

$$d_{norm} = \frac{(d_i - r_i^{vdw})}{r_i^{vwd}} + \frac{(d_e - r_e^{vdw})}{r_e^{vwd}}$$

where r_i^{vdW} and r_e^{vdW} are the van der Waals radii of the atoms. The value of d_{norm} is negative or positive depending on intermolecular contacts being shorter or longer than the van der Waals separations. The parameter d_{norm} displays a surface with a red−white−blue color scheme, where bright red spots highlight shorter contacts, white areas represent contacts around the van der Waals separation, and blue regions are devoid of close contacts. For a given crystal structure and set of spherical atomic electron densities, the Hirshfeld surface is unique[8] and thus it suggests the possibility of gaining additional insight into the intermolecular interaction of molecular crystals.

The Hirshfeld surfaces of both complexes have been mapped over d_{norm} (range -0.1 Å to 1.5 Å) (Figure S2); shape index and curvedness (Figure S3). Graphical plots of the molecular Hirshfeld surfaces mapped with d_{norm} used a red-white-blue colour scheme, where red highlights shorter contacts, white is used for contacts around the Van der Walls separation, and blue is for longer contacts. The intense circular depressions (deep red) seen on the surfaces indicates the hydrogen bonding contacts. The small extent of area and light colour on the surface indicates weaker and longer contact other than hydrogen bonds.

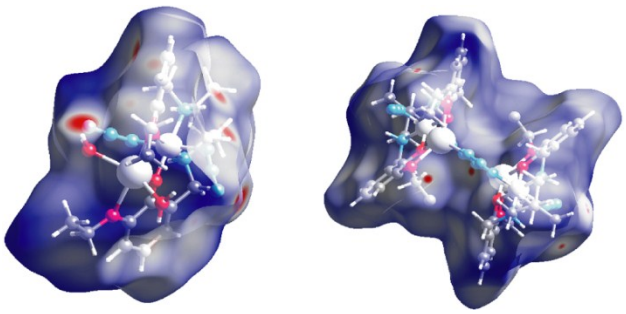

Figure S2: Hirshfeld surfaces mapped with d_{norm} for complexes **1** (left) and **2** (right).

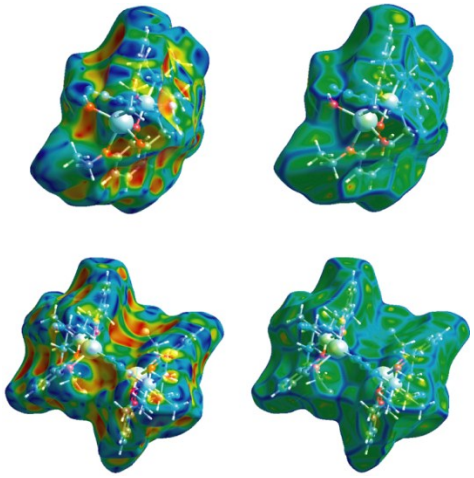

Figure S3: Hirshfeld surfaces mapped over shape index (left) and curvedness (right) for complexes **1** (top) and **2** (bottom).

Two-dimensional fingerprint plots obtained from Hirshfeld surface analysis may also be useful to shed light on the supramolecular interactions. Intermolecular interactions appear as distinct spikes in this plot. Complementary regions are observable in the two-dimensional fingerprint plots where one molecule act as donor ($d_e > d_i$) and the other as an acceptor ($d_e < d_i$).

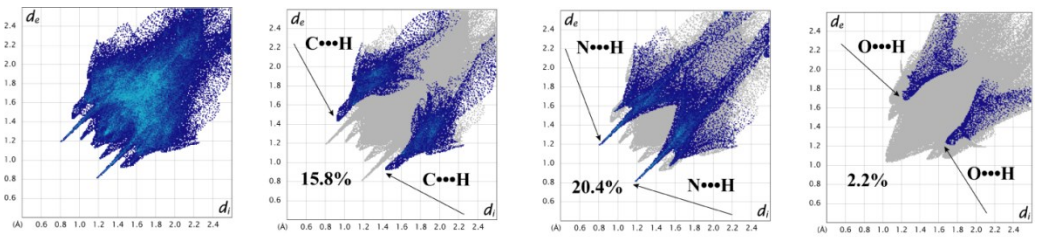

Figure S4: Fingerprint plot: Full (left), resolved into H···C/C···H (second from the left), H···N/N···H (second from the right) and H···O/O···H (right) contacts contributed to the total Hirshfeld Surface area of complex **1**.

In the fingerprint plot of complex **1** (Figure S4), the most dominant interactions are found for N···H/H···N contacts, which contribute to 20.4% of the total Hirshfeld surface and C···H/H···C which contribute to 15.8%, while contribution of interactions coming from O···H contacts are very less i.e. 2.2%. This result also supports that the fact that most of the supramolecular interactions involve N···H hydrogen bonding and C-H···π interactions. The fingerprint plot of complex **2** (Figure S5) shows that C···H/H···C interactions are major contributor (22.0%) of total Hirshfeld Surface area, although H···N/N···H interactions also has a good contribution (17.0%).

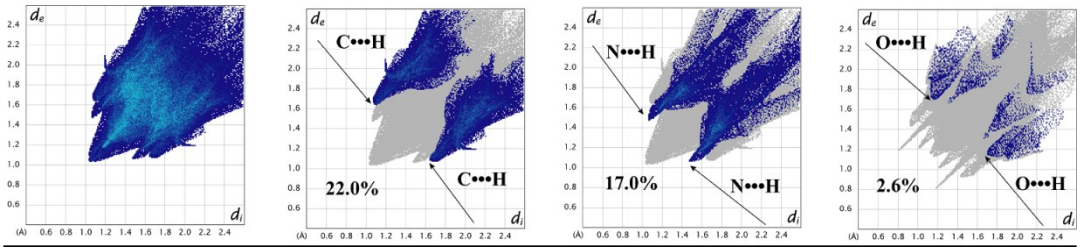

Figure S5: Fingerprint plot: Full (left), resolved into H···C/C···H (second from the left), H···N/N···H (second from the right) and H···O/O···H (right) contacts contributed to the total Hirshfeld Surface area of complex **2**.

At this moment, it is significant to construct a histogram of relative areas for comparing the supramolecular interactions in these two complexes (**1** and **2**) in different chemical environments. Therefore the percentage contributions of significant atom-type/atom-type contacts to the Hirshfeld surfaces for both complexes have been depicted in Figure S5 in the form of histograms, which clearly indicate that supramolecular interactions involving N···H hydrogen bonding and C-H···π interactions are significant in solid state structure, although N···H

hydrogen bonding is more dominant in complex **1** whereas the key interaction in complex **2** is C-H···π interaction.

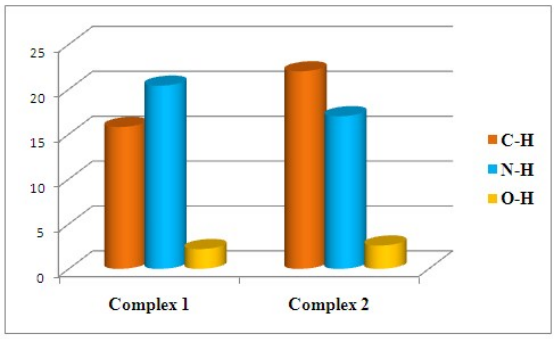

Figure S6: Percentage contributions to the Hirshfeld surface area for significant close intermolecular contacts in complexes **1** and **2**.

Table S1: Selected bond angles (°) of complexes **1** and **2**.

Complex	**1**	**2**
O(1)-Co(1)-O(2)	82.5(3)	80.7(2)
O(1)-Co(1)-N(1)	96.4(3)	91.1(2)
O(1)-Co(1)-N(2)	177.4(3)	173.7(3)
O(1)-Co(1)-N(3)	91.2(3)	92.2(3)
O(1)-Co(1)-N(6)	91.0(3)	90.6(3)
O(2)-Co(1)-N(1)	176.6(3)	171.8(2)
O(2)-Co(1)-N(2)	96.5(3)	93.2(3)
O(2)-Co(1)-N(3)	92.9(3)	93.3(3)
O(2)-Co(1)-N(6)	89.1(3)	89.7(3)
N(1)-Co(1)-N(2)	84.8(3)	95.0(3)
N(1)-Co(1)-N(3)	83.9(3)	87.8(3)
N(1)-Co(1)-N(6)	94.1(3)	89.5(3)
N(2)-Co(1)-N(3)	91.2(4)	86.6(3)
N(2)-Co(1)-N(6)	86.6(3)	90.9(3)

N(3)-Co(1)-N(6)	177.2(4)	176.1(3)
O(5)-Co(2)-O(6)	-	81.3(2)
O(5)-Co(2)-N(11)	-	90.3(3)
O(5)-Co(2)-N(12)	-	172.5(3)
O(5)-Co(2)-N(13)	-	93.2(3)
O(5)-Co(2)-N(14)	-	92.2(3)
O(6)-Co(2)-N(11)	-	91.7(3)
O(6)-Co(2)-N(12)	-	91.3(3)
O(6)-Co(2)-N(13)	-	174.1(3)
O(6)-Co(2)-N(14)	-	92.1(3)
N(11)-Co(2)-N(12)	-	89.5(3)
N(11)-Co(2)-N(13)	-	90.3(3)
N(11)-Co(2)-N(14)	-	175.6(3)
N(12)-Co(2)-N(13)	-	94.3(3)
N(12)-Co(2)-N(14)	-	88.3(3)
N(13)-Co(2)-N(14)	-	86.1(3)
O(1)-Na(1)-O(2)	65.8(3)	66.4(2)
O(1)-Na(1)-O(3)	61.3(3)	69.5(2)
O(1)-Na(1)-O(4)	122.6(3)	133.0(3)
O(1)-Na(1)-O(5)	89.9(3)	-
O(1)-Na(1)-O(6)	126.6(6)	-
O(1)-Na(1)-N(9)	-	130.2(3)
O(2)-Na(1)-O(3)	121.1(3)	125.3(3)
O(2)-Na(1)-O(4)	64.3(3)	68.9(2)
O(2)-Na(1)-O(5)	124.9(4)	-
O(2)-Na(1)-O(6)	97.9(6)	-
O(2)-Na(1)-N(9)	-	140.9(3)
O(3)-Na(1)-O(4)	174.3(3)	130.8(3)
O(3)-Na(1)-O(5)	79.3(3)	-
O(3)-Na(1)-O(6)	93.7(5)	-

O(3)-Na(1)-N(9)	-	92.8(3)
O(4)-Na(1)-N(9)	-	94.3(3)
O(4)-Na(1)-O(5)	96.2(4)	-
O(4)-Na(1)-O(6)	86.9(5)	-
O(5)-Na(1)-O(6)	133.8(7)	-
O(5)-Na(2)-O(6)	-	67.0(2)
O(5)-Na(2)-O(7)	-	68.8(2)
O(5)-Na(2)-O(8)	-	125.4(3)
O(5)-Na(2)-N(8)	-	140.0(3)
O(6)-Na(2)-O(7)	-	132.8(2)
O(6)-Na(2)-O(8)	-	69.0(2)
O(6)-Na(2)-N(8)	-	131.2(3)
O(7)-Na(2)-O(8)	-	129.6(3)
O(7)-Na(2)-N(8)	-	93.9(3)
O(8)-Na(2)-N(8)	-	93.8(3)

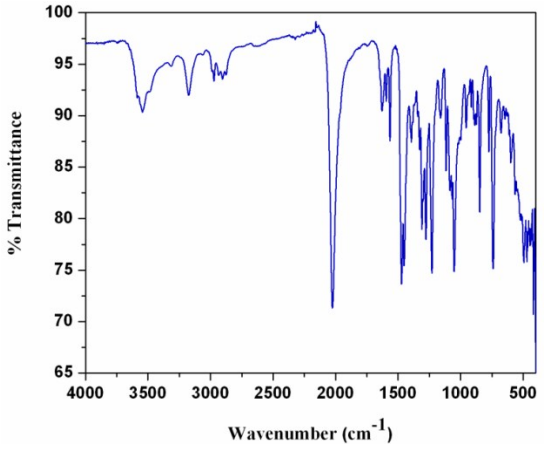

Figure S7: IR spectrum of complex **1**.

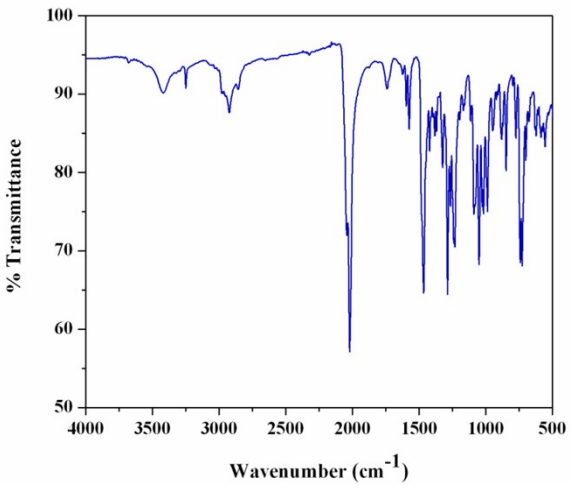

Figure S8: IR spectrum of complex **2**.

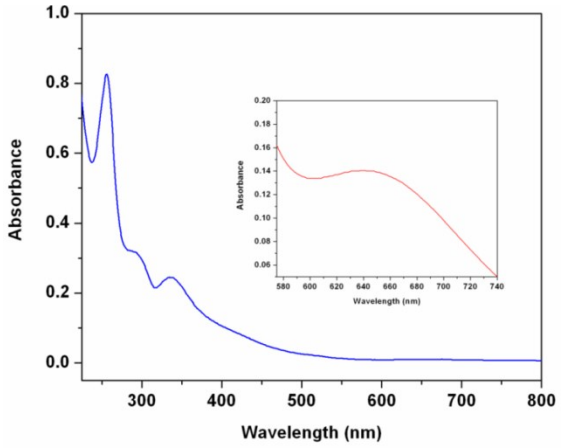

Figure S9: Electronic spectrum of complex **1**. Inset shows the selected small range (550-750 nm) electronic spectrum of the complex.

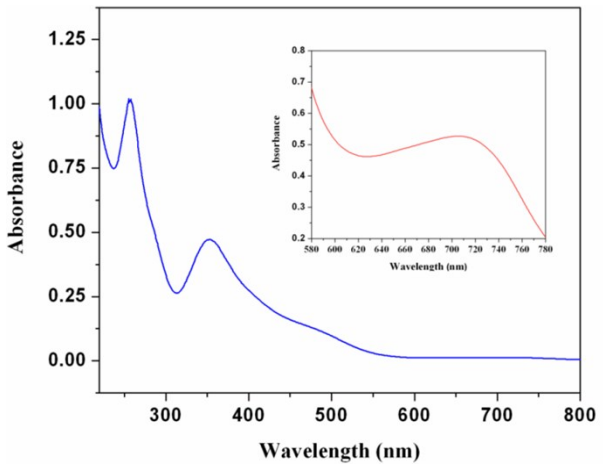

Figure S10: Electronic spectrum of complex **2**. Inset shows the selected small range (550-750 nm) electronic spectrum of the complex.

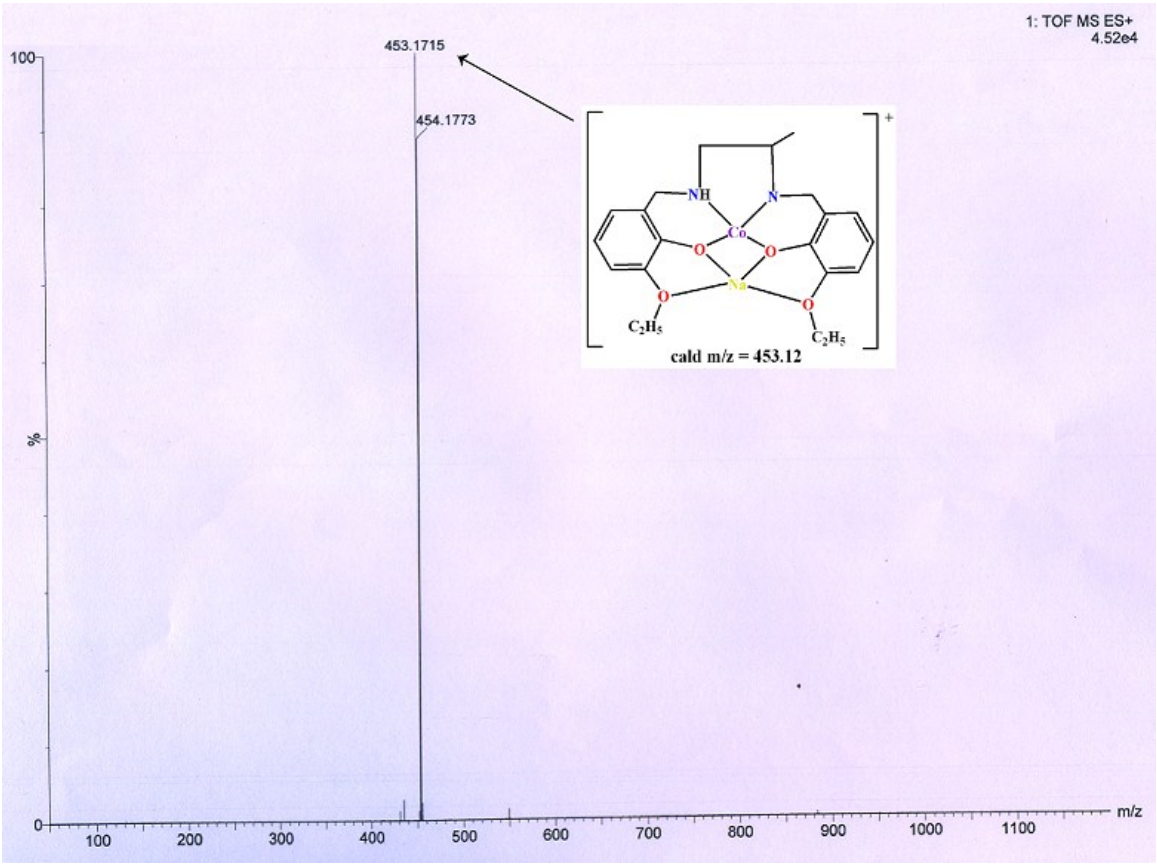

Figure S11: ESI-MS positive spectrum of complex **1** in acetonitrile medium at room temperature.

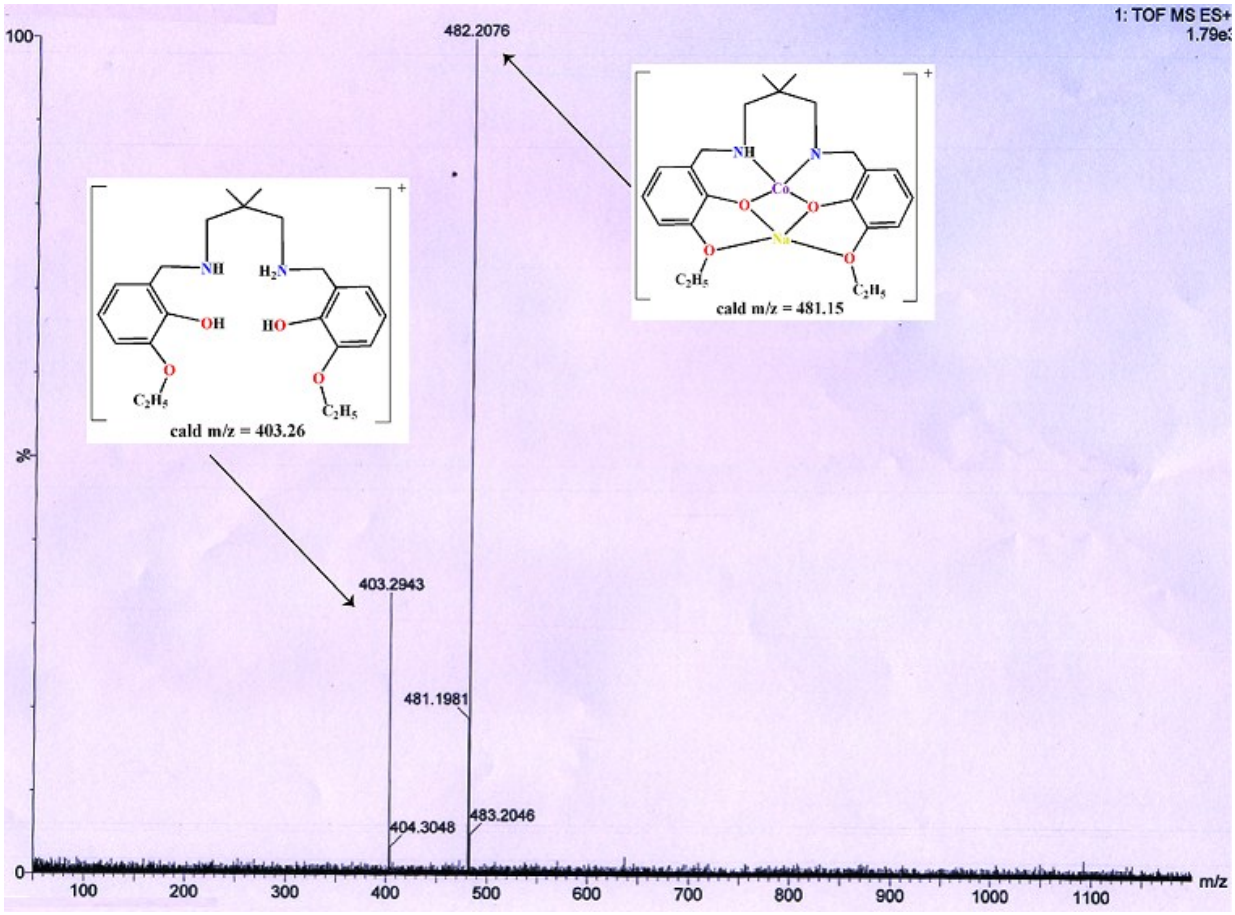

Figure S12: ESI-MS positive spectrum of complex **2** in acetonitrile medium at room temperature.

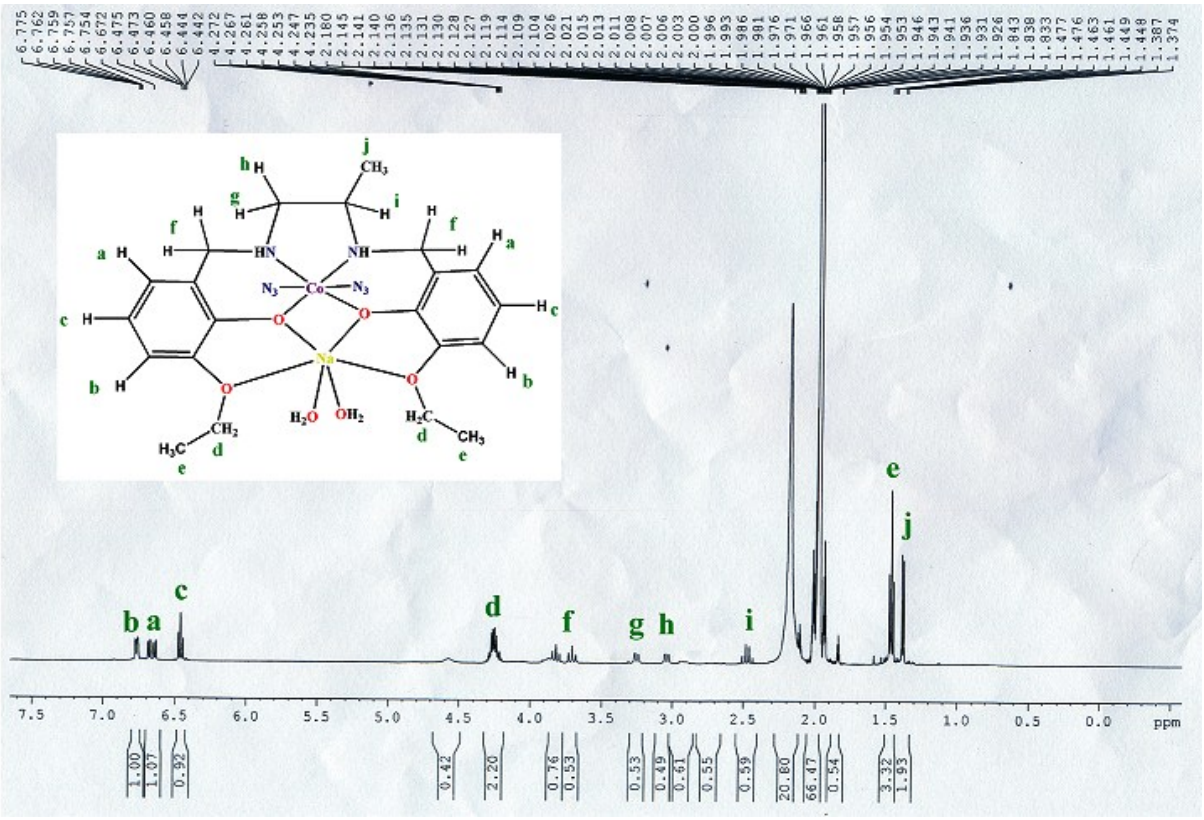

Figure S13: ^{1}H NMR spectrum of complex **1** in CD_3CN at room temperature.

References

1 M. A. Spackman and D. Jayatilaka, *CrystEngComm,*2009, **11**, 19-32.

2 F. L. Hirshfeld, *Theor. Chim. Acta,* 1977, **44**, 129-138.

3 A. L. Rohl, M. Moret, W. Kaminsky, K. Claborn, J. J. McKinnon and B. Kahr, *Cryst. Growth Des.*, 2008, **8**, 4517-4525.

4 A. Parkin, G. Barr, W. Dong, C. J. Gilmore, D. Jayatilaka, J. J. McKinnon, M. A. Spackman and C. C. Wilson, *CrystEngComm*, 2007, **9**, 648-652.

5 M. A. Spackman and J. J. McKinnon, *CrystEngComm*, 2002, **4**, 378-392.

6 S. K. Wolff, D. J. Grimwood, J. J. McKinnon, D Jayatilaka, M. A. Spackman, Crystal Explorer 2.0; University of Western Australia: Perth, Australia, 2007. http://hirshfeldsurfacenet.blogspot.com/.

7 F. H. Allen, O. Kennard, D. G. Watson, L. Brammer, A. G. Orpen and R. J. Taylor, *J. Chem. Soc. Perkin Trans.2*, 1987, S1-S19.

8 J. J. Kinnon, M. A. Spackman, A. S. Mitchell, *Acta Cryst.*, 2004, **B60**, 627-668.